Supporting Information

Protein-polyelectrolyte complexes to improve the biological activity of proteins in layer-by-layer assemblies

Aurélien vander Straeten, Anna Bratek-Skicki, Loïc Germain, Cécile d'Haese, Pierre Eloy, Charles-André Fustin, Christine Dupont-Gillain*

Turbidimetry and UV dosage

After centrifugation at 380 g, lysozyme is mainly found in the supernatant when (-)/(+net)=2 (Figure S1). This is in contrast with the result obtained after centrifugation at 9500 g (see Figure 1a). For values around of (-)/(+net) around 1.5 however, lysozyme is mostly found in the pellet even after centrifugation at 380 g. This indicates that PPCs size decreases at (-)/(+net)=2 compared to (-)/(+net)=1.5.

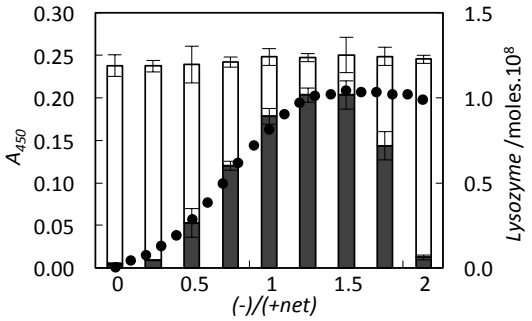

Figure S1. Normalized absorbance of a lysozyme solution undergoing PSS_l addition in such a way that negative-to-positive charge ratio varies between 0 and 2 at pH 7.5 in HEPES buffer. Lysozyme amount assessed by UV spectrophotometry in the pellet (■) and in the supernatant (□) after PPCs centrifugation at 380 g for 15 min.

X-ray photoelectron spectroscopy (XPS)

The sequential adsorption of PPCs with (-)/(+net)=2 with PAH enables multilayer construction. In order to assess lysozyme presence in these multilayered systems, XPS experiments were performed on a Kratos Axis Ultra spectrometer (Kratos Analytical – Manchester – UK) using the procedure described elsewhere.[1] Glass surfaces coated with a thick layer of either PAH or PSS_h prepared by evaporation of a concentrated solution were first analyzed by XPS as control samples. The following assemblies were then built on a PAH-PSS_h bilayer cushion: [PAH-PSS_l]$_5$ and [PAH-PPCs_2]$_5$. C1s, N1s and S2p spectra are presented in Figure S2 for (i) PAH, (ii) PSS_h, (iii) [PAH-PSS_h]$_2$-[PAH-PSS_l]$_5$ and (iv) [PAH-PSS_h]$_2$-[PAH-PPCs_2]$_5$. For PAH, Figure S2 (i) shows a C1s peak that is attributed mainly to two components at 284.8 eV and 286.2 eV, respectively corresponding to aliphatic carbon chains (**C**-C,H) and amine groups (**C**-N).[2] The N1s peak can also be decomposed in two components at 399.5 eV and 401.3 eV that are attributed respectively to nitrogen in amine or amide groups, and to protonated nitrogen.[3] A very small S2p contamination is also detected. For the PSS_h sample (Figure S2 (ii)), the C1s peak can be decomposed with a main component corresponding to aliphatic and aromatic carbon (**C**-C,H). Another peak corresponding to the aromatic shake-up is observed at 292.1 eV. It also appears that no N1s peak is detected, and that a peak corresponding to the S2p doublet from PSS sulfonate groups is observed, which can be decomposed in two components at 168.4 eV and 169.6 eV.[4] Table S1 highlights that, as expected, Cl^- is detected as PAH counter ion and Na^+ as PSS counter ion with a good consistency since 14.1% Cl is detected together with 13.7% total N in PAH samples, and 8.1% Na is detected for 8.2% S in PSS_h samples.

Then, multilayers were analyzed. Figure S2 (iii) shows spectra for [PAH-PSS_h]$_2$-[PAH-PSS_l]$_5$. Two components at 284.8 eV and 286.2 eV, respectively corresponding to aliphatic carbon (**C**-C,H) and amine groups (**C**-N) were detected in the C1s peak for [PAH-PSS_l]$_5$ multilayers.

For multilayers integrating PPCs, i.e. $[PAH\text{-}PSS_h]_2$-[PAH-PPCs_2]$_5$ in Figure S2 (iv), a component corresponding to the peptide link is detected at 288.1 eV in the C1s peak. In addition, a higher total nitrogen content together with less protonated nitrogen compared to $[PAH\text{-}PSS_h]_2$-$[PAH\text{-}PSS_l]_5$, and a new component at 163.9 eV in the S2p peak, corresponding to thiols from cysteines, strongly indicate protein presence. Regarding PSS marker, the S2p peak at 167.9 eV confirms PSS detection. Finally, the remaining protonated component in the N1s peak supports PAH presence. In order to assess each species contribution, one can compute a $[\underline{\mathbf{C}}\text{-}(C,H)]_{lysozyme}/[N\text{-}\underline{\mathbf{C}}\text{=}O]_{lysozyme}$ of 1.7 for lysozyme based on its sequence (P00698) and thus assume that 7%×1.7=11.7% of the **C**-(C,H)] component is due to proteins. Then, based on the sulfonate surface atomic concentration detected and the PSS formula, one can assess that PSS contributes up to 3.1%×8=24.8% of the **C**-(C,H) component. PAH is thus expected to contribute to $[\underline{\mathbf{C}}\text{-}(C,H)]_{PAH} = [\underline{\mathbf{C}}\text{-}(C,H)]_{tot} - [\underline{\mathbf{C}}\text{-}(C,H)]_{lysozyme} - [\underline{\mathbf{C}}\text{-}(C,H)]_{PSS}$=41.6%-11.7%-24.8%=5.1% of the **C**-(C,H) component. In order to confirm the contributions of PAH and lysozyme to the detected **C**-(C,H) component, one can correlate it to the nitrogen peak decomposition. Indeed, 5.3% of **C**-(C,H) measured for PAH theoretically gives 1.8% (5.3%×1/3) protonated nitrogen (**C**-(C,H)/NH^+=3) and a close 2.1% is detected. Regarding lysozyme, 11.7% of **C**-(C,H) theoretically gives 8.1% N (based on lysozyme sequence, **C**-(C,H)/N=1.4) and in agreement with the value of 8.1% found experimentally. It can thus be concluded, based on C1s peak decomposition and on the correlation with other peaks, that proteins, PSS and PAH are all three present in the probed volume of $[PAH\text{-}PSS_h]_2$-[PAH-PPCs_2]$_5$ samples (analysed depth ~10 nm).

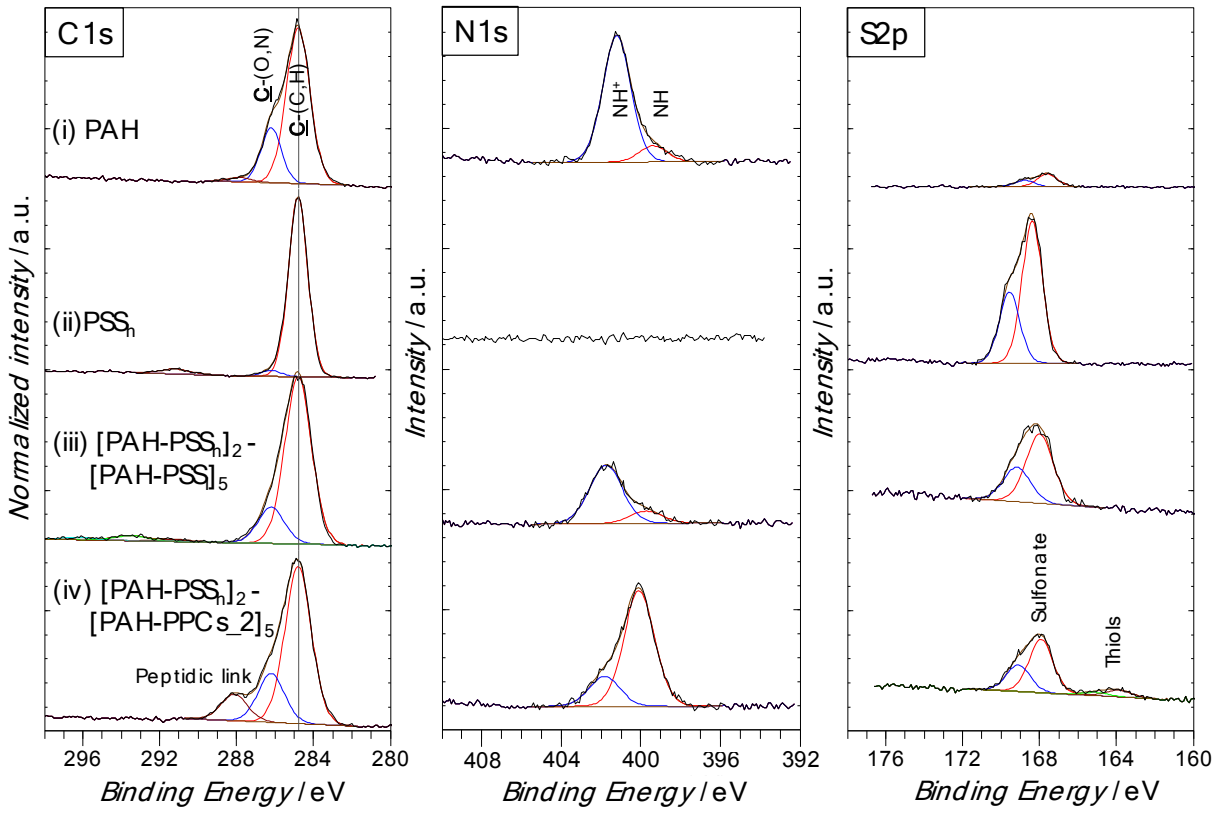

Figure S2. C1s, N1s and S2p peaks recorded by X-ray photoelectron spectroscopy (XPS) for glass surfaces coated with (i) PAH, (ii) PSS_h or with a $[PAH\text{-}PSS_h]_2$ cushion followed by (iii) $[PAH\text{-}PSS_l]_5$ and (iv) [PAH-PPCs_2]$_5$. Spectra are presented with their respective decomposition in components or doublets. The C 1s peaks were normalized in such a way that their maxima, i.e. **C**-(C-H) component, have the same height. Peak intensities can thus not be directly compared.

Table S1. Surface atomic concentration (in %, excluding H) obtained by X-ray photoelectron spectroscopy (XPS) on glass surfaces coated with (i) PAH, (ii) PSS_h, or a $[PAH\text{-}PSS_h]_2$ cushion followed by (iii) $[PAH\text{-}PSS_l]_5$ and (iv) $[PAH\text{-}PPCs\_2]_5$. bdl: below detection limit. C_{shup}: aromatic shake-up

	O 1s	NH+	NH	C_{shup}	N-**C**=O	**C**-(O,N)	**C**-(C,H)	C_{tot}	S_{thiol}	$S_{Sulfonate}$	Si	Na	Cl
PAH	3.6	12.2	1.5	bdl	1.4	15.4	50.9	67.7	bdl	0.7	0.3	bdl	14.1
PSS_h	18.8	bdl	bdl	2.7	bdl	2.0	58.9	63.6	bdl	8.2	0.9	8.1	0.3
$[PAH\text{-}PSS_l]_5$*	22.7	3.8	0.9	1.8	bd	9.6	44.6	56.0	bdl	4.4	12	0.2	bdl
$[PAH\text{-}PPCs]_5$	18.1	2.1	8.1	bdl	7.0	12.9	41.6	61.5	0.4	3.1	6.7	bdl	bdl

*0.4% K is also detected for $[PAH\text{-}PSS]_5$

3D-printed reactor for the measurement of enzymatic activity

The 3D-printed reactors were built by fused deposition modelling in Carbon Black poly(lactic acid) (Machines-3D, France) with a Replicator 2X 3D printer (Makerbot, Germany). The nozzle and the plate were respectively heated to 220 °C and 60 °C. Cylinders of 15 mm diameter and 70 mm length were printed with one shell and a linear infill of 30%. Hence, the developed surface was estimated to be around 320 cm^2. The reactors were inserted and sealed into a thermoretractable sheath and connections with tubing were insured by A-Lok reducing unions placed at both ends (see Figure S3). After coating with multilayers, they were placed vertically into a thermostatic bath and a *Micrococcus lysodeikticus* (1 g L^{-1}) suspension was circulated at 5 mL min^{-1} from a buffering vessel to the reactor (from the bottom to the top, i.e. orange arrow in Figure S3). Absorbance of the suspensions at 450 nm was then recorded at the reactor outlet in a continuous flow spectrophotometric cell. The microorganism suspension was recirculated through the buffering vessel, the reactor and the spectrophotometric cell for 400 min.

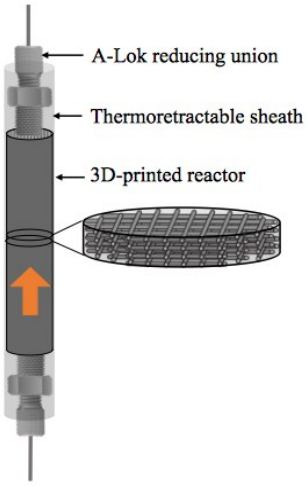

Figure S3. Scheme of the 3D-printed reactor and representation of the infill pattern. The orange arrow shows the flow direction.

References of the Supporting Information section

1 M.F. Delcroix, S. Laurent, G.L. Huet, C. Dupont-Gillain, *Acta Biomaterialia* 2015, **11**, 68.
2 P. M. Dietrich, T. Horlacher, P.-L. Girard-Lauriault, T. Gross, A. Lippitz, H. Min, T. Wirth, R. Castelli, P. H. Seeberger, W. E. S. Unger, *Langmuir* 2011, **27**, 4808.
3 J. M. C. Lourenço, P. A. Ribeiro, A. M. Botelho do Rego, F. M. Braz Fernandes, A. M. C. Moutinho, M. Raposo, *Langmuir* 2004, **20**, 8103.
4 Beamson, G.; Briggs, D., *J. Chem. Educ.* 1993, **70**, A25.